EPJ Web of Conferences **59**, 01003 (2013)
DOI: 10.1051/epjconf/20135901003
© Owned by the authors, published by EDP Sciences, 2013

Ignition tuning for the National Ignition Campaign

O. Landen[1,a], J. Edwards[1], S.W. Haan[1], J.D. Lindl[1], T.R. Boehly[2], D.K. Bradley[1], D.A. Callahan[1], P.M. Celliers[1], E.L. Dewald[1], S. Dixit[1], T. Doeppner[1], J. Eggert[1], D. Farley[1], J.A. Frenje[5], S. Glenn[1], S.H. Glenzer[1], A. Hamza[1], B.A. Hammel[1], C. Haynam[1], K. LaFortune[1], D.G. Hicks[1], N. Hoffman[3], N. Izumi[1], O.S. Jones[1], J.D. Kilkenny[6], J.L. Kline[3], G.A. Kyrala[3], A.J. Mackinnon[1], J. Milovich[1], J. Moody[1], N. Meezan[1], P. Michel[1], D.H. Munro[1], R.E. Olson[4], J. Ralph[1], H.F. Robey[1], A. Nikroo[6], S.P. Regan[2], B.K. Spears[1], L.J. Suter[1], C.A. Thomas[1], R. Town[1], D.C. Wilson[3], B.J. MacGowan[1], L.J. Atherton[1] and E.I. Moses[1]

[1] *Lawrence Livermore National Laboratory, PO Box 5508, Livermore, CA 94550, USA*
[2] *Laboratory for Laser Energetics, Rochester, NY, USA*
[3] *Los Alamos National Laboratory, Los Alamos, NM, USA*
[4] *Sandia National Laboratory, Albuquerque, NM, USA*
[5] *Plasma Science and Fusion Center, MIT, Cambridge, MA 02139, USA*
[6] *General Atomics, San Diego, CA, USA*

Abstract. The overall goal of the indirect-drive inertial confinement fusion [1] tuning campaigns [2] is to maximize the probability of ignition by experimentally correcting for likely residual uncertainties in the implosion and hohlraum physics [3] used in our radiation-hydrodynamic computational models, and by checking for and resolving unexpected shot-to-shot variability in performance [4]. This has been started successfully using a variety of surrogate capsules that set key laser, hohlraum and capsule parameters to maximize ignition capsule implosion velocity, while minimizing fuel adiabat, core shape asymmetry and ablator-fuel mix.

1. INTRODUCTION TO TUNING PARAMETERS AND PLATFORMS

The 20 key adjustable laser, capsule and hohlraum parameters for tuning indirect-drive ignition are shown in Figure 1, divided amongst the four implosion attributes of fuel adiabat, implosion velocity, core symmetry and mix between ablator and fuel and hotspot. Figure 2 shows the experimental platforms used to measure and set these parameters, and example data. Fuel adiabat is minimized by setting optimum velocities and merge depths of the four shocks measured using D_2–filled capsules and a re-entrant ("Keyhole") VISAR system [5, 6] by changing the power level and timing of each section in the laser power profile. Implosion velocities and the rocket-model-associated ablator mass remaining are measured using backlit x-ray radiography of the capsule limb [7] and can be adjusted using the peak power level, ablator thickness and dopant choice. Implosion symmetry is inferred from the soft x-ray reemission limb uniformity of a surrogate high Z sphere at early time ("Reemit") [8] and from core x-ray self-emission at pole and equator views at bangtime [9, 10], and optimized using a combination

[a] e-mail: landen1@llnl.gov

This is an Open Access article distributed under the terms of the Creative Commons Attribution License 2.0, which permits unrestricted use, distribution, and reproduction in any medium, provided the original work is properly cited.

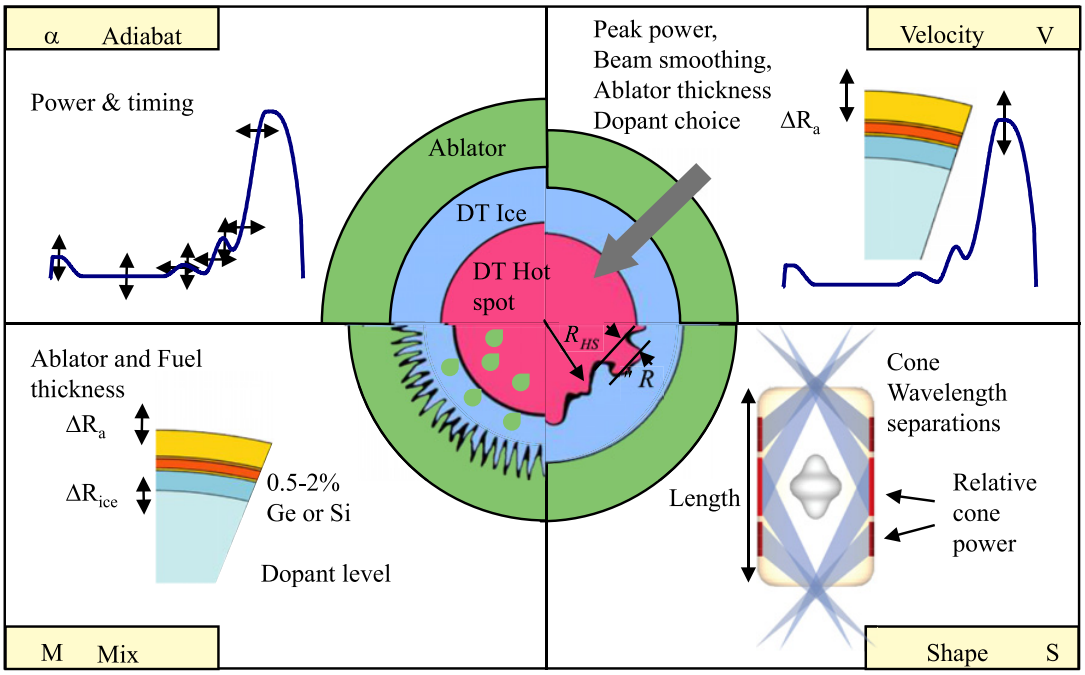

Figure 1. Quad chart depicting the 4 main parameters (adiabat, shape, velocity and mix) that are set by varying key hohlraum, capsule and laser parameters.

of hohlraum length, time-dependent incident cone balance, and wavelength separation between beam cones altering crossbeam power transfer [11]. Hot spot mix is inferred using absolutely calibrated Ge dopant spectroscopy [12].

2. TUNING STRATEGY

Figure 3 illustrates the optimized tuning sequence in tabular form. Each observable (row) is primarily responsible for setting one or more of the laser, capsule and hohlraum tuning parameters (column), shown as the main diagonal boxes. Off-diagonal dependencies exist, but only those above the diagonal require iteration, major examples of which are shown as arrows. We have almost completed two tuning iterations so far, and have varied every parameter except the ablator and fuel thickness. We start with the time-integrated full pulse "symmetry capsule" implosion platform to check and initially set the time-integrated core symmetry and drive. We then begin tuning the time-dependent adiabat and symmetry using truncated pulses. We recheck the time-integrated symmetry, then evaluate the peak velocity and mass remaining, the latter affecting the expected ablator cold-fuel mix [3]. In between, we test performance using intentionally yield-dudded THD cryogenic layered implosions [13] that provide yield, fuel ρr from the neutron downscattered ratio (dsr), a check on core shape, and ablator and filltube mix in the hotspot.

3. TUNING PRECISIONS, ACCURACIES AND RESULTS

Table 1 shows that we have met the required precision for all baseline platforms and associated measurements, both for tuning and checking implosion performance. We have also met or are close to meeting the tuning accuracy required. For example, the first shock timing campaign set the shock

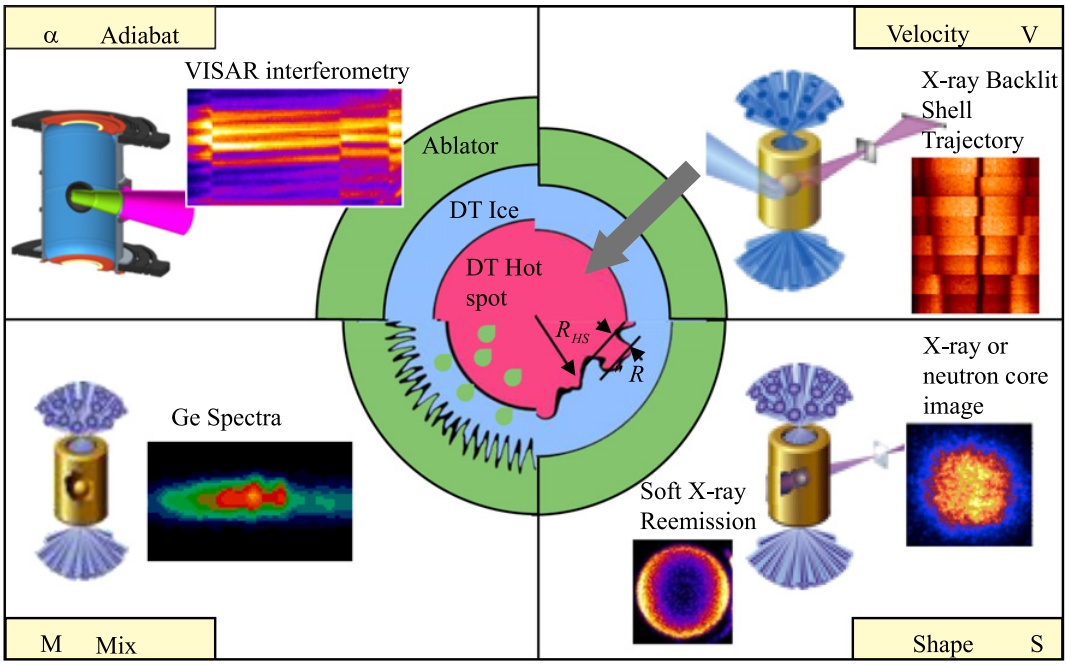

Figure 2. Quad chart depicting the variety of platforms and observables, examples of which are shown.

strengths and merge depths to within 1.5× of ignition tolerance in just 5 shots, leading to a predicted fuel adiabat of 1.5. An additional tolerable increase of 3% in adiabat due to hot electron preheat is inferred from absolute measurements of the >100 keV capsule Bremsstrahlung [14]. The peak capsule velocities have reached 95 ± 5% of required by switching to Si-doped plastic capsules and extending the drive pulse, though leaving 1–1.5% less ablator mass than optimum. The symmetry campaign set the low (<6) mode asymmetry (intrinsic and random, including both polar Legendre and azimuthal modes) to typically ±7 μm rms, also within 1.5× of ignition tolerance. This included significantly modifying the first picket inner vs outer cone power balance to account for crossbeam transfer from outer to inner cone beams in the laser entrance hole (LEH) window plasma. The contribution from midmode perturbations is currently estimated as small from the initial measured fuel ice uniformity. In the absence of other direct measurements, the cold fuel ablator mix is inferred from the ablator mass remaining. The x-ray spectrometer viewing Ge 2-1 line emission inferred 1.5–2× less than the 75 ng of ignition-tolerable hotspot mix in the cryogenically-layered CHGe implosions.

To better quantify the progress in optimizing adiabat α, peak fuel velocity v, weighted low and midmode rms shape perturbation $\Delta R_{hotspot}/R_{hotspot}$, ablator mix fraction in fuel $(1\text{-}M_{clean}/M_{DT})$, and hot spot mix in ng, we use the Ignition Threshold Factor (ITF) [3]. It relates the measured or inferred quantities to the calculated probability of ignition, with ITF = 1 representing 50% probability.

$$ITF = 3.6\left(\frac{v}{370\,\mathrm{km/s}}\right)^{8}\left(\frac{\alpha}{1.40}\right)^{-4}\left(1-1.2\frac{\Delta R_{hotspot}}{R_{hotspot}}\right)^{4}\left(\frac{M_{clean}}{M_{DT}}\right)^{0.5}\left(1-\frac{CHGe_{.005}\,\mathrm{ng}}{450\,\mathrm{ng}},\frac{CHSi_{.01}\,\mathrm{ng}}{600\,\mathrm{ng}}\right). \quad (1)$$

To quantify the progress in implosion performance, we use an ICF version of the Lawson criterium, denoted ITFx [4], which is expressible below in terms of the no burn DT-equivalent neutron yield and

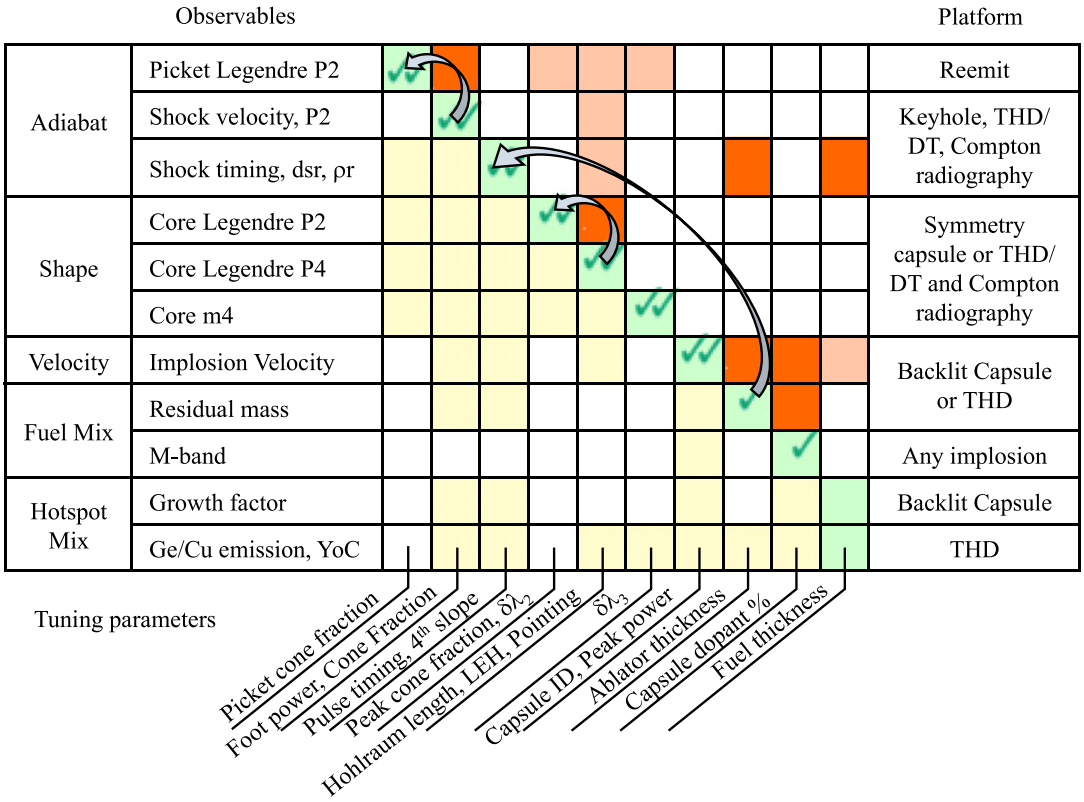

Figure 3. Tabular view of tuning campaign sequence depicting the key observables and platforms as rows vs. the key target and laser tuning parameters as columns. The boxes on the diagonal depict which observable sets which tuning parameters, the boxes below and above the diagonal depict which observables will be affected by tuning parameters set earlier (later) in the sequence, the latter requiring iterations, especially for the stronger cross-couplings shown in dark shade. Check marks depict what has been completed so far.

the dsr representing the measure of fuel ρr:

$$ITFx = \left(\frac{Yield}{3.2e15}\right)\left(\frac{dsr}{0.07}\right)^{2.3}. \tag{2}$$

Figure 4(a) displays in bar chart format the inferred ITF factors for each of the terms in Eq. (1), including error bars, for two CHGe and two CHSi implosions of increasing incident laser energy. Where no information is available (such as hot spot mix for CHSi capsules), we use calculated cross-sensitivities based on other measured parameters such as mass remaining. Also included as open bars are the allocated values [3] to reach an acceptable minimum ITF of 1.3 for an ignition attempt. We note the improvements in time are mainly in the implosion velocity by switching to lower albedo Si-doped CH ablator. As the laser energy is increased to 1.6 MJ, one sees that the increase in velocity is partially offset by an increase in predicted mix due to less ablator mass remaining. Clearly, more measurements are required (and planned) to reduce uncertainties, principally in the velocity and mix areas.

Figure 4(b) plots the ITF and ITFx per Eqs. (1) and (2) for those 4 shots, showing an increasing trend in both. Before tuning, ITFx was .002, so we have seen an almost 50× improvement, principally due to increased laser energy and shock timing doubling the dsr to .05. One expects ITF to be below ITFx for small (<0.5) values of both. The fact that ITF is consistently higher than ITFx suggests we

Table 1. Precision and accuracy of goal met relative to budget and ignition tolerance for key parameters.

		Precision		Accuracy or Goal	
Platform	**Key Parameter**	**Budget**	**Aug-11**	**Spec**	**Aug-11**
Reemit	Picket Symmetry (P2)	±3%	±1%	±7.5%	±2%
Keyhole	Shock Velocities	±2%	±1.5 − 2%	±5%	±4%
	Shock Merge Depths	±4 μm	±3 − 5 μm	±6 μm	±9 μm
Backlit Capsule	Velocity (Gated)	±5%	±5%	±2%	±5%
	Velocity (Streaked)	±1.5%	±1.5%	±2%	Await 4 w comb
	Mass Remaining	±1.5%	±1%	±1.5%	±1.5%
	Hydroinstability Growth Factor	±20%	Designed	±20%	
Symmetry Capsule	Hot Spot Symmetry rms	±5 μm	±3 μm	±5 μm	±7 μm
	Peak Drive (Dante)	±5%	±3%	±5%	Not Appropriate
	X-ray Bangtime	±50 ps	±30 ps	±50 ps	±50 ps
	Hot electrons @ Capsule	±50 J	±50 J	<100 J	<100 J
	X-ray preheat fraction	±10%	±7%	±10%	±7%
	Hot spot mix (ng CHGe)	±30 ng	±20 ng	<75 ng	Await inner dopant
Cryo-Layered Capsule (THD and DT)	Yield (Neutron Time-of-Flight (nToF), Activation)	±5%	±5%	±10%	±10%
	Fuel ρr (Magnetic Recoil Spectrometer)	±10%	±8%	±10%	±8%
	Tion (nToF)	±10%	±7%	±10%	Bulk motion bias
	Nuclear Bangtime (Gamma Reaction History)	±50 ps	±50 ps	±50 ps	±50 ps
	Nuclear Burn Duration (GRH)	±30 ps	±15 ps	±30 ps	±15 ps
	Hot Spot radius (P0) (Neutron Imaging (NI))	±5 μm	±3 μm	±5 μm	±3 μm
	Fuel radius (P0) (NI)	±5 μm	±3 μm	±5 μm	±5 μm
	Fuel ρr rms (Compton Radiography)	±10%	±15%, OMEGA	±10%	±15%

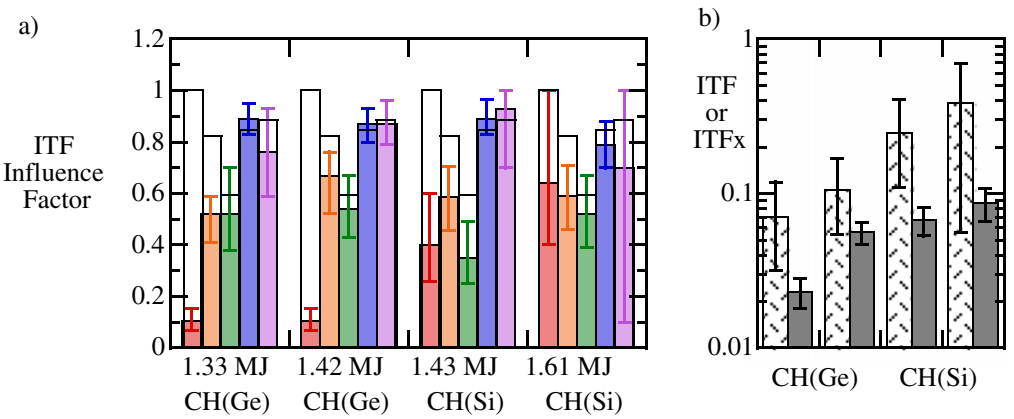

Figure 4. a) Measured ITF factor bar chart for velocity, adiabat, shape, cold mix and hotspot mix respectively, compared to ignition allocation (open bars) for four 1.3–1.6 MJ CH(Ge) and CH(Si) shots b) Inferred ITF (striped) and measured ITFx (grey) bar chart for these four cryogenic layered implosions.

may be missing an indicator of performance degradation in ITF such as midmode fuel-hotspot mix or higher adiabat due to a 5^{th} shock. It is also by comparing ITF to ITFx that we can become alerted to tuning platform surrogacy issues, possible code modelling deficiencies requiring dedicated experiments isolating a particular physics issue (such as averaged treatment of multiple species plasmas), or the need for more tuning platforms. If we suspect the implosion performance is more sensitive to a given parameter than modelling predicts, then we will experimentally check that sensitivity.

4. SUMMARY AND FUTURE WORK

All the baseline tuning and ignition performance platforms have now been qualified at NIF, and meet precision requirements. Two rounds of a tuning campaign have led to many changes in laser and target parameters, including some unanticipated (hohlraum diameter changed from 5.44 to 5.75 mm to improve symmetry tunability, wavelength separation applied between 23° and 30° beams to reduce m = 4 mode). We have reached an ITF of 0.39 ± 0.3, and an ITFx of 0.085 ± 0.015, with both increasing with time.

More tuning and performance platforms are in the process of being validated. In the area of active probes, these include a dual axis VISAR to set the 2^{nd}–4^{th} shock pole-to-equator symmetry, 75–100 keV point-projection Compton radiography [15] of the fuel size, shape and ρr uniformity using 2 quads of NIF, backlit x-ray radiography of ablation front growth of surface divots and bumps to assess Rayleigh-Taylor growth rates, backlit implosion velocity and thickness measurements of the ablator early in the pulse and in cryogenically-layered implosions to check EOS and the presence of a fifth shock, with the added potential to view the low Z fuel interfaces by refraction-enhanced imaging [16]. In the area of passive probes, these include using Au-lined higher albedo U hohlraums to improve hohlraum efficiency [17, 18], codoping the CHSi capsules with trace amounts of Ge and Cu for assessing hot spot mix emanating from throughout the inner ablator region as one varies the ablator and fuel thickness and Si dopant level to vary the interface Atwood number, and using I as a radiochemical tracer of mix.

This work was performed under the auspices of the U.S. Department of Energy by Lawrence Livermore National Laboratory under Contract DE-AC52-07NA27344.

References

[1] J.D. Lindl, P. Amendt, R.L. Berger, *et. al*., Phys. Plasmas **11**, 339 (2004)
[2] O. L. Landen, J. Edwards, S.W. Haan, *et. al*., Phys. Plasmas **18**, 051002 (2011)
[3] S.W. Haan, J.D. Lindl, D.A. Callahan, *et. al*., Phys. Plasmas **18**, 051001 (2011)
[4] M.J. Edwards, J.D. Lindl, B.K. Spears, *et. al*., Phys. Plasmas **18**, 051003 (2011)
[5] T.R. Boehly, V.N. Goncharov, W. Seka, *et. al*., Phys. Rev. Lett. **106**, 195005 (2011)
[6] H.R. Robey, P.M. Celliers, J.L. Kline, *et. al*., Phys. Rev. Lett. **108**, 215004 (2012)
[7] D. A. Callahan, N. B. Meezan, S. H. Glenzer, *et. al*., Phys. Plasmas **19**, 056305 (2012)
[8] E.L. Dewald, J. Milovich, C. Thomas, *et. al*., Phys. Plasmas **18**, 092703 (2011)
[9] G.A. Kyrala, J.L. Kline, S. Dixit, *et. al*., Phys. Plasmas **18**, 056307 (2011)
[10] R.P.J. Town, M.D. Rosen, P.A. Michel, *et. al*., Phys. Plasmas **18**, 056302 (2011)
[11] P. Michel, S.H. Glenzer, L. Divol, *et. al*., Phys. Plasmas **17**, 056305 (2010)
[12] S.P. Regan, R. Epstein, B.A. Hammel, *et. al.*, Phys. Plasmas **19**, 056307 (2012)
[13] A.J. Mackinnon, J.L. Kline, S.N. Dixit, *et. al.*, Phys Rev. Lett. **108**, 215005 (2012)

[14] T. Doeppner, C.A. Thomas, L. Divol, *et. al.*, Phys. Rev. Lett. **108,** 135006 (2012)
[15] R. Tommasini, S.P. Hatchett, D.S. Hey, *et. al*., Phys. Plasmas **18,** 056309 (2011)
[16] J. Koch, O.L. Landen, B.J. Kozioziemski, *et. al*., J. Appl. Phys. **105**, 1 (2009)
[17] J.L. Kline, S.H. Glenzer, R.E. Olson, *et. al*., Phys. Rev. Lett. **106**, 085003 (2011)
[18] S.H. Glenzer, B.J. MacGowan, N.B. Meezan, *et. al*., Phys. Rev. Lett. **106**, 085004 (2011)